Automated Extraction of Forest Road Network Geometry from Aerial LiDAR

Storm J.C. Beck, Michael J. Olsen, John Sessions, Michael G. Wing[*]

Oregon State University, Peavy Hall 280, Corvallis, OR 97333, USA

Abstract

We developed an algorithm that was designed to create a spatial database of a forested transportation network using aerial LiDAR. The algorithm uses two main attributes, LiDAR intensity values and ground return density. The road extraction process was developed using aerial LiDAR from McDonald-Dunn Research Forest near Corvallis, Oregon, U.S.A. The road extraction process requires X, Y, Z coordinates, intensity values, canopy type, and the maximum road grade. To compare the results of the process, nine road segments were field surveyed with terrestrial LiDAR. The result of the road extraction process resulted in 80% true positives, 34% false positives, 20% false negatives, and 38% true negatives in identifying forest roads. The average absolute value difference in the road width between the two data sets were 1.1m, while the cut/fill slope differences were minimal (> 4%) and the difference in road cross slope was two percent. These results were comparable with other published studies that examined differences between LiDAR measurements and field measurements.

1. Introduction

The ability of vehicles to navigate the transportation network is based on both vehicle and roadway characteristics. Roadway characteristics that influence vehicle accessibility are road width, curve radius, curve widening, length of curve, cross slope, vehicle overhang and road edge obstructions. These characteristics are especially important when evaluating vehicles of non-standard dimensions, such as pole trailers and chip vans. These non-standard (typically larger) vehicles allow for the transportation of high valued products (utility poles) or the transportation of low valued products (chips or hogfuel) and provide opportunities for the forest industry to increase economic value from forests. Currently, two methods are used when determining if a non-standard vehicle can access a forest site: (1) field measurements and (2) visual inspection by the trucking contractor. Both of these methods can be time consuming and typically only evaluate portions of the transportation network. We investigate a method in which forest roads and geometry can be identified and extracted from aerial LiDAR data to evaluate the accessibility of non-standard vehicles in the forest transportation network.

Several studies have evaluated the horizontal and vertical accuracy of using aerial LiDAR data for forest road measurements. Rieger et al. (1999) approached mapping forest roads to create breaklines for more accurate Digital Terrain Model (DTM) creation. White et al. (2010) used a hill-shade approach to map forest roads in the Santa Cruz Mountains, California. Craven et al. (2011) used different methods including hand digitization of the road centerline from LiDAR intensity and point cloud images. LiDAR intensity is a measure of the return strength of laser pulses and is dependent on the reflectivity of a surface (Figure 1). In addition to the hand digitization, an algorithm was created to identify the road centerline from an initial estimate of its location. White et al. (2010) and Craven et al. (2011) produced similar results with road centerline differences less than 2 meters of the field surveyed centerlines.

While prior work has been able to detect centerlines, few studies have looked at identifying forest roads from intensity values and density of returns, which could yield improved results. Craven et al. (2011) used intensity images for the identification of forest roads but did not use return densities to help in the identification process. This study builds upon previous work to examine the use of both intensity values and return densities to identify and extract forest roads.

Figure 1. Intensity return map of a forested area in the McDonald Forest.
(The image is colored by intensity values: dark = low to light = high)

2. Materials and methods
2.1 Extraction form Aerial LiDAR Data Sets

In this study, the process in which forest roads were extracted from LiDAR data sets was based on two fundamental properties:

1) Intensity values on forest roads will be significantly different than those on the forest floor as intensity values change with material properties (Figure 2) (Jenson, 2007).

2) The density of ground returns on forest roads will be higher than those on the forest floor, as canopy cover over a forest road is typically less than the canopy cover over the forest floor (Jenson, 2007). This enables more LiDAR returns to penetrate all the way through the canopy and reflect off of the road surface.

Figure 2 describes the workflow and algorithms developed to extract forest road networks.

Since diverse canopy conditions can occur along forest roads, it is necessary to recognize the corresponding acceptable ranges of intensity values for forest roads under various canopy types.

Three canopy types were chosen with the assumption that the intensity values of ground returns would vary enough between each to require identifying different intensity value ranges for roads under these three canopy conditions. The canopy types include:

(1) Clear cuts or Meadows - The forest road is clearly visible with no to minimal obstructions from the flight altitude.

(2) Young Forests - An even-aged forest between 15 and 35 years old with the road as an open corridor surrounded by a closed canopy. These forests have not yet created a closed canopy structure over the roadway, but create a uniform layer on both sides of the road between 15-45 feet tall in which return penetration is difficult and few ground returns are obtained.

(3) Mature Forests - Resembling older forest structure, with large, dominate trees with understory growth. The canopy cover over a forest road will have areas with gaps visible from the flight altitude and areas that are completely closed in by the surrounding trees and vegetation.

Read in
X,Y,Z,I Data

Step n in {G}
if $i_{min} < n_{iv} > i_{max}$
$n_{iv} \to$ {RL}

Step i in{RL}
Step n in {G}
If $0.78 \geq \sqrt{(n_x - i_x)^2 + (n_y - i_y)^2}$; count n
$n_{dist} = \sqrt{(n_x - i_x)^2 + (n_y - i_y)^2}$
If $n_{dist} \leq 0.78$ & count n ≥ 2
$n \to$ {RL}

Step i in{RL}
Step n in {G}
$n_{dist} = \sqrt{(n_x - i_x)^2 + (n_y - i_y)^2}$
If $n_{dist} \leq 10.67$
$n \to$ {RL}

Step i in{RL}
Step n in {G}
$n_{dist} = \sqrt{(n_x - i_x)^2 + (n_y - i_y)^2}$
count $n_{dist} \leq sr_2$
If count $\leq thres_2$
remove i from {RL}

Step i in{RL}
Step n in {G}
$n_{dist} = \sqrt{(n_x - i_x)^2 + (n_y - i_y)^2}$
count if $n_{dist} \leq sr_1$
If count $\leq thres_1$
remove i from {RL}

Create a grid
Step z in {GRID}
Step p in {GRID}
if $\Delta \geq \sqrt{(z_{xc} - p_{xc})^2 + (z_{yc} - p_{yc})^2}$
$p \to$ {Z_{ADJ}}

Step z in {GRID}
Step i in {RL}
$n_{dist} = \sqrt{(z_{xc} - i_x)^2 + (z_{yc} - i_y)^2}$
If $n_{dist} \leq \Delta$
$z \to$ {$GRID_{RL}$}

Step z in {GRID}
Step p in {Z_{ADJ}}
If p in {$GRID_{RL}$}
count p;
If count p ≤ 20
Remove p from {$GRID_{RL}$} & {RL}

Step w in {GRID}
Step p in {Z_{ADJ}}
If p in {$GRID_{RL}$} $\to$ {w}{p};

Step w in {w}{p}
Step p in {w}{p}

Step t in {t}{o}
Step o in {t}{o}
$t_{dist} = \sqrt{(wp_{xc} - to_{xc})^2 + (wp_{yc} - to_{yc})^2}$

Step p in {Z_{ADJ}}
$n_{dist} = \sqrt{(p_{xc} - wp_{xc})^2 + (p_{yc} - wp_{yc})^2}$
If $n_{dist} < t_{dist}$

$n_{slope} = (\bar{p_z} - w_{pz})/(n_{dist})$

If $n_{dist} < min_{dist}$ & $n_{slope} < m_{grade}$

$p \to$ {$GRID_{RL}$}

Step z in {GRID}
Step i in {RL}
$n_{dist} = \sqrt{(z_{xc} - i_x)^2 + (zy_c - iy)^2}$
If $n_{dist} \leq csize$
$z \to$ {$GRID_{RL}$}

Step i in{RL}
Step n in {G}
$n_{dist} = \sqrt{(n_x - i_x)^2 + (n_y - i_y)^2}$
If $n_{dist} \leq 10.67$
$n \to$ {RL}

Print out {RL}
(X,Y,Z,I)

Create a Delaunay
Triangulation of the RL

Create a grid
Step f in {GRID}
$f = DT_{elv}$ @ f_{xc}, f_{yc}

RL = Roaded list
i_{min} = Minimum acceptable intensity value
i_{max} = Maximum acceptable intenstiy value
ADJ = Adjacent
DT_{elv} = Delaunay triangulation
$GRID_{RL}$ = Road list of the grid
Δ = Cell size
m_{grade} = Maximum road grade
-> = Place into set

min_{dist} = Minimum distance
{RL} = Set of points in the roaded list
{G} = Set of all ground points
{GRID} = Set of cells within the grid of the area
{Z_{ADJ}} = Set of cells that are adjacent to cell Z
{w}{p} = Set of cells that are connected to cell w
wp_{yc} = The y coordinate of the center of the cell
connected to cell
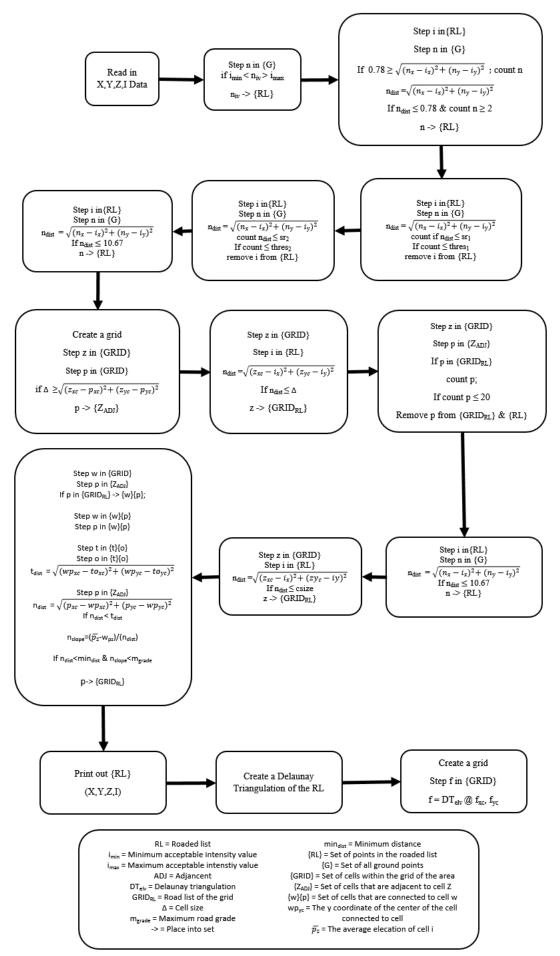$\bar{p_z}$ = The average elecation of cell i

Figure 2. The workflow for the road extraction process.

The acceptable intensity value ranges (Table 1) for the different canopy types were determined through experimentation; and as such, these ranges are specific to this dataset. The determination of these values must balance obtaining enough returns along the road while minimizing the number of returns throughout the forest floor. The following steps describe the preprocessing required to obtain these ranges for each system.

Step (1): Filter LiDAR data to have only ground returns. The ground filtering method that was used for our data was performed by Watershed Sciences (Watershed Sciences, 2008) using a combination of commercial software, custom algorithms, and manual processing developed for the Pacific Northwest.

Step (2): Obtain a starting range of intensity values for each cover type. Subsets of points were selected along segments of forest roads and the distribution of the intensity values was determined that were associated with the ground returns. The intensity values that contained the majority of the returns were selected as the starting range(s) (Figure 3).

Step (3): Determine if the range(s) of intensity values were too broad for each cover type. If this was the case, the range(s) would then be adjusted until the returns selected were primarily on the forest road producing a semi-continuous forest road selection and clumped or scattered non-forest road selections (Figure 4).

Table 1. The determined intensity value ranges for identifying roaded areas.

Canopy Type	Intensity Value Range
Clear Cut or Meadow	2 - 30
Young Forest	15 - 50
	130 - 140
Mature Forest	40 - 80
	140 - 170

Acceptable intensity values were spread out across the entire area and not just constrained to forest roads (Figure 4). LiDAR return density was used to further to distinguish roaded areas from non-roaded areas (Figure 5). Several search radii were used to locate areas of higher return densities and processed these areas to differentiate them from non-roaded areas. This process involved two road properties, (1) forest roads will have a higher ground return density than the surrounding areas and (2) forest roads are continuous and do not have breaks. A filter was determined based on these road properties to remove isolated areas of high return densities and to connect long enough segments of identified roaded areas together to create a continuous forest transportation network (henceforth referred to as the connection routine).
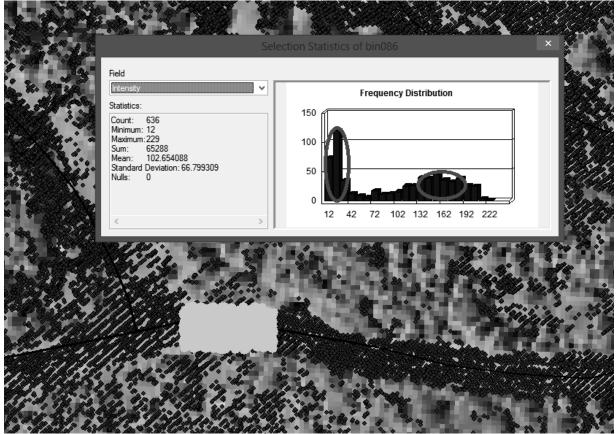

Figure 3. The second step in identifying an acceptable intensity value ranges for each cover type.
(The circles indicate the ranges in which a majority of the points fall within,
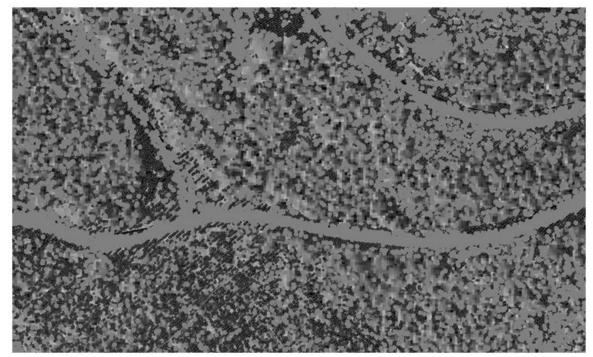this is where a fine tuning of the ranges started)

Figure 4. The third step in the pre-processing steps of selecting appropriate intensity value ranges for various canopy types.
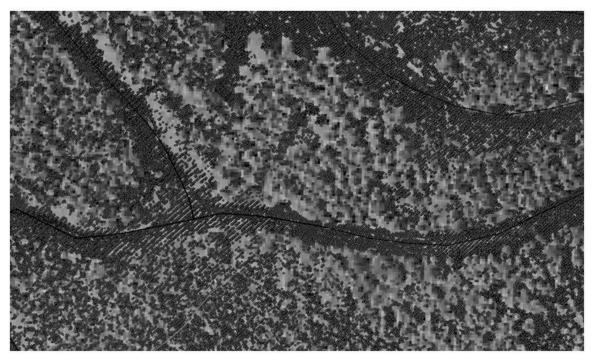

Figure 5. An illustration of the high ground return density along a forest road compared to the surrounding forest floor.

It was identified during the development of this algorithm that a connection routine was need to fill in the gaps between identified roaded areas. To develop the connection routine the authors used forest road attributes: maximum forest road slope and maximum distance between road segments. To determine acceptable segments to join together, a recursive algorithm was used. This process evaluated all of the neighboring cells to determine if they were an acceptable addition to the solution based on slope and shortest path. A grid was created of the study area and each cell was identified if it contained at least one roaded return (Figure 6) based on the previous criteria. After identifying all satisfactory cells, continuous segments of these roaded cells were identified. If the number of connected grids were less than 20, all returns within those cells were removed from the roaded list to remove short, isolated areas from the solution (cells marked "O" in Figure 6). Next, the algorithm adds cells back into the solution to connect isolated road segments, based on the assumption that forest roads are continuous and are not isolated. This process used a
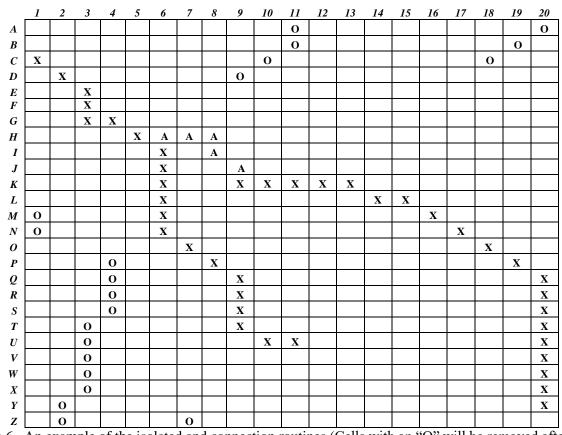
	1	2	3	4	5	6	7	8	9	10	11	12	13	14	15	16	17	18	19	20
A											O									O
B											O								O	
C	X									O								O		
D		X							O											
E			X																	
F			X																	
G			X	X																
H					X	A	A	A												
I						X		A												
J						X			A											
K						X			X	X	X	X	X							
L						X								X	X					
M	O					X										X				
N	O					X											X			
O							X											X		
P			O					X											X	
Q			O						X											X
R			O						X											X
S			O						X											X
T			O						X											X
U			O							X	X									X
V			O																	X
W			O																	X
X			O																	X
Y		O																		X
Z		O					O													

Figure 6. An example of the isolated and connection routines (Cells with an "O" will be removed after the isolation routine and the cells with an "A" will be added after the connection routine).

shortest path connection routine with a constraint that no cell could be added to the solution if the slope between the two cells is greater than the maximum road grade that the user inputted. This step prevented the algorithm from adding a cell that created a slope greater than the maximum road grade (cells designated by "A" in Figure 6).

After this process was completed, a Delaunay triangulation DTM (Bourke, 1989) of the roaded list was created and rasterized, which is subsequently converted into a grid by extracting elevation values at fixed intervals in X and Y. Finally, an ASCII clear-text file of the roaded list in X, Y, Z, I format is exported.

2.2 Terrestrial LiDAR Data Collection

Six road systems throughout the McDonald-Dunn Forest were identified as possible candidates for validation of the aerial LiDAR results, excluding areas of activity between 2008 and 2012. These road systems were categorized by cover type and road surface via an on-site field investigation.   From this, three road systems were selected to be used in the analysis because they would be examples of the best and worst potential of road geometry extraction.

The road segments were surveyed using a FARO FOCUS3D laser scanner and six sphere targets that were 152.4 mm in diameter and made of a highly reflective and durable matte-white polyester. For each

sample, scans were completed at a resolution of 0.006 degrees, approximately 20 m apart alternating opposite sides of the road edge. All of the six spheres were placed within 30 m of the scanner for registration proposes.

Three control points were set during the data collection, one at the start, middle, and end of each road segment. A spherical target was centered on top of the control points and leveled using a bipod and a five second level bubble. Depending on the canopy cover, the control points were either surveyed using a total station which was tied to two static GPS observations (one to start the traverse from and one to set the backsight) or each of the control points were directly surveyed using static GPS observations with Topcon HiperLite + GPS receiver. The GPS receivers observed for at least eight hours, sometimes longer depending on sky plot visibility. The Online Positioning User Service (OPUS) was used to post process all GPS observations (Soler et al., 2006).

The scan registration process used a least-squares adjustment to register the spherical targets within each scan together and to perform a 6 parameter rigid body transformation of the scans to the control points to geo-reference the data. The average errors on the control points were 5.0 cm for the start control point, 3.2 cm for the middle control point, and 8.4 cm for the end control point (Beck, 2014).

2.3 Statistically Filtering Terrestrial LiDAR Data Sets

After registering the terrestrial LiDAR data sets, vegetation was removed via a filter to be able to compare the road prisms of the terrestrial and aerial data. A majority of the vegetation within the scans were manually clipped out. To improve results, a statistical filter was used to filter out the remaining vegetation, which was based on the BIN 'N' GRID process (Olsen, 2011).

Two enhancements were made to the BIN 'N' GRID process to help remove non-ground returns on the edges of the scan area or in areas where the amount of ground returns were minimal due to scan placement and vegetation. On the edges of the scan area, the terrestrial scanner has a difficult time obtaining returns from the ground due to the scan angle and surrounding vegetation and topography. This is evident when setting up the scanner on the cut slope side of the road (Figure 7). In such a configuration, the scanner obtains few returns from the fill slope due to its inability to see the entire fill slope. In addition to visibility limitations, this process also removes areas of the scan in which more returns were obtained from vegetation than from the ground.

The first enhancement was a comparison between elevation of the ith cell ($Z_{i,\Delta}$) computed with the user's defined grid cell size (Δ) and the value at that location based on a one meter grid cell size ($Z_{i,1m}$). A one meter grid cell size provided a balance of maintaining original data integrity on the road and removing vegetation along the edge of the road prism. The road prism includes not only the road surface, but also the extents of the ditches or cut and fill slopes that are connected to the road surface. To ensure that the comparison process did not coarsen the data, a buffer of 3m was applied to ensure that $Z_{i,1m}$ was lower than any of the elevations from the corresponding user defined cell size cells ($Z_{i,\Delta}$) by three meters prior to overwriting the elevation values based on the user input cell size (Equation 1).

$$Z_{i,\Delta} = Z_{i,1m} \; if \; Z_{i,\Delta} > (Z_{i,1m} + 3m) \qquad (1)$$

The second enhancement compares the $Z_{i,\Delta}$ to elevations of the neighboring cells for consistency. The average elevation ($\bar{Z}_{i,j\Delta}$) and standard deviation ($\sigma_{i,j\Delta}$) of the neighboring cells (j) surrounding the ith cell were computed using Equations 2 and 3:

$$\bar{Z}_{i,j\Delta} = \frac{1}{n_j} \sum_{j=1}^{n_j} Z_{j\Delta} \qquad (2)$$

$$\sigma_{i,j\Delta} = \sqrt{\frac{\sum_{j=0}^{n_j} (z_{j,\Delta} - \overline{z_{i,j\Delta}})^2}{(n_j - 1)}} \qquad (3)$$

where $Z_{j,\Delta}$ = the elevation of the jth neighboring cell where $j \neq i$ with a cell size Δ and n_j = number of neighboring cells j

$Z_{j\Delta}$ is reduced if it has a higher elevation than the mean plus the standard deviation of the elevations of the neighboring cells, as determined by Equation 4.

$$Z_{i,\Delta} = \bar{Z}_{i,j\Delta} \; if \; Z_{i,\Delta} \geq \bar{Z}_{i,j\Delta} + \sigma_{i,j\Delta} \qquad (4)$$

These enhancements were incorporated into a statistical filtering program, enabling the user to select which of the seven statistical processes they wanted to use for creating the Digital Elevation Model (DEM): (1) minimum, (2) maximum, (3) mean, (4) standard deviation, (5) special (see Equation 5), (6) special with neighborhood, (7) median or (8) create grids for all of the modes. The comparison enhancement (Equation 1) was a part of every mode, while the neighborhood comparison (Equations 2-4) was only part of process six.

$$Z_{i,\Delta} = \bar{Z}_{i,\Delta} \; if \; \sigma_{u,\Delta} > \sigma_{,i\Delta}$$
$$else \; Z_{i,\Delta} = \bar{Z}_{i,\Delta} - N * \sigma_{i,\Delta} \qquad (5)$$

where $\sigma_{u,\Delta}$ = the user inputted standard deviation and N = the user defined number of standard deviations.

After inputting the statistical filtering process, the user inputs the desired cell size, Δ and if needed the standard deviation threshold, $\sigma_{u,\Delta}$ and the number of standard deviations, N. The user is then prompted for an optional quality control verification using control point elevations and the filtered data. After the completion of the process, four output files can be created: (1) floating point grid file, (2) statistical file, (3) projection file, and (4) the quality control verification difference file.

After visual inspections of the various statistical filtering processes, the fifth process was used. This process determined the elevation of each cell, $Z_{i,\Delta}$ as the average elevation if the standard deviation, $\sigma_{i,\Delta}$, was less than the user inputted standard deviation, $\sigma_{u,\Delta}$. However, if the standard deviation, $\sigma_{i,\Delta}$, was greater than the user inputted standard deviation, $\sigma_{u,\Delta}$, the elevation of the cell, $Z_{i,\Delta}$, would be the average elevation, $\bar{Z}_{i,\Delta}$, minus the number of standard deviation, N, times the standard deviation, $\sigma_{i,\Delta}$.

The final elevation of each cell, $Z_{i,\Delta}$, was determined by running the comparison process (Equation 1). The results of this process removed vegetation while maintaining the detail of the data along the fill and cut slopes. (3)
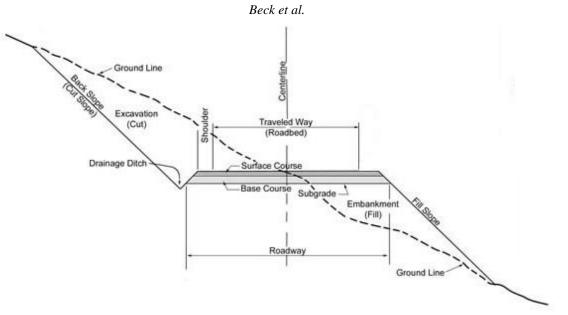
Figure 7. Typical forest road cross-section for a cut and fill section.

After inputting the statistical filtering process, the user inputs the desired cell size, Δ and if needed the standard deviation threshold, $\sigma_{u,\Delta}$, and the number of standard deviations, *N*.   The user is then prompted for an optional quality control verification using control point elevations and the filtered data.   After the completion of the process, four output files can be created: (1) floating point grid file, (2) statistical file, (3) projection file, and (4) the quality control verification difference file.

After visual inspections of the various statistical filtering processes, the fifth process was used. This process determined the elevation of each cell, $Z_{i,\Delta}$ as the average elevation if the standard deviation, $\sigma_{i,\Delta}$, was less than the user inputted standard deviation, $\sigma_{u,\Delta}$. However, if the standard deviation, $\sigma_{i,\Delta}$, was greater than the user inputted standard deviation, $\sigma_{u,\Delta}$, the elevation of the cell, $Z_{i,\Delta}$, would be the average

elevation, $\bar{Z}_{i,\Delta}$, minus the number of standard deviation, N, times the standard deviation, $\sigma_{i,\Delta}$. The final elevation of each cell, $Z_{i,\Delta}$, was determined by running the comparison process (Equation 1). The results of this process removed vegetation while maintaining the detail of the data along the fill and cut slopes.

2.4 Road Geometry Extraction

With the two data sets filtered to only include road prism returns, transects were created through the data to obtain cross-section views of the road segment to extract road prism variables using the TopCAT toolbar in ArcGIS (Olsen et al., 2012). In TopCAT, transects were created every 5 m along a centerline and points were created every 0.5 m along each transect; XYZ coordinates were created for all points. The profiles provided the ability to evaluate the differences and consistency between the aerial and terrestrial data sets (Figure 8).
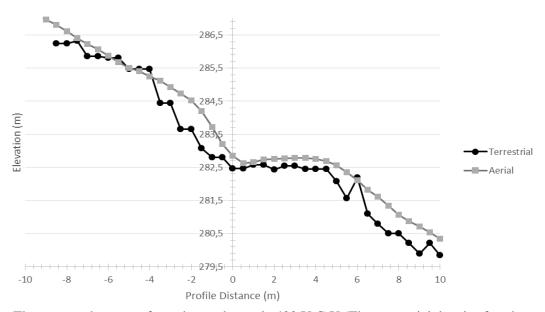

Figure 8. The extracted transect from the road sample 400 Y G Y (The terrestrial data is after the statistical filtering process, and the aerial data is the data from the road extraction process).

3. Results and Discussion

3.1 Road Extraction form Aerial LiDAR Data

Once the road extraction process was ran on all of the sample sites, the percentage of the extracted road segments were calculated (Table 2). The extraction process successfully extracted 67 percent of the road prisms that were field sampled with a terrestrial scanner. However, the process had a difficult time extracting native surface roads, as evidenced by the 21 percent extraction on sample 410 O D Y and the zero percent extraction on site 240 C D Y. If these two sites were removed; the road prism extraction process would successfully identify 84 percent of the road prisms that were field sampled.

The major contributing factor of identifying non-roaded areas when using the road extraction program was the extreme change of the canopy cover through the processed area (Figures 9 and 10 A). The road segment of interest (400 O G N) in this area was located in a mature canopy type with the maximum road grade of 10 percent (Figure 10 B). The outcome of the road extraction was 47 percent but the majority of the area was identified as roaded (Figure 10 A and Figure 10 B). The southern half of the area is a farm field, which has higher point densities and different intensity values than the mature canopy type (Figure 10 B). This difference in canopy covers in the study area proved to be a weakness of the road extraction process, which requires relative consistency of cover type for the intensity thresholds.

Table 2. The road extraction results compared to the field measured road segments (sorted by surface type than by covertype)

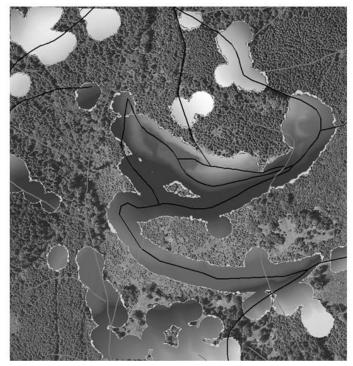| Segment Name	Length of road sample (m)	Length of road segment found by the extraction process (m)	Percentage
260 O G Y 2	181.1	169.5	94%
260 O G Y	240.7	109	45%
420 O G N	224.7	224.7	100%
400 O G N	205.1	96	47%
400 M G N	237	237	100%
400 Y G Y	308.3	308.3	100%
400 C G Y	209.7	209.7	100%
410 O D Y	184.7	38.1	21%
240 C D Y	149.7	0	0%
		Average	67%

Figure 9. The identified roaded areas of the forest road extraction process for a young canopy cover and a maximum road grade of 20 percent (The shaded areas are the results of the extraction process overlaid on an orthophoto of the area. The young canopy cover is found in the center of the image, producing minimal gaps in road identification. The gaps increase due to the differing canopy covers).
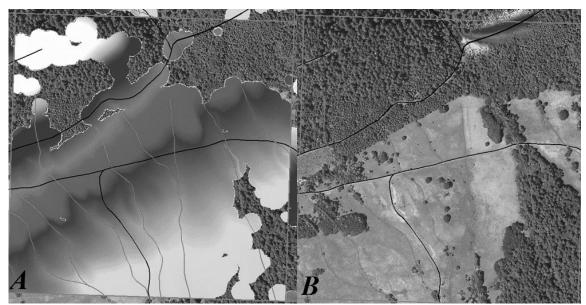
Figure 10. (A) The areas identified (shaded areas) as roaded using the road extraction process for a mature cover type with a 10 percent maximum road grade, (B) The terrestrial road segment 400 O G N (upper right corner of the image) that was of interest when running the road extraction process shown in A.

To further evaluate the effectiveness of the algorithm, false positives, false negatives, and true negatives were evaluated (Table 3). These attributes were evaluated on an area basis, due to the difficulty of determining lengths of non-roaded segments. The mean true positive was 81%, false positive 49%, false negative 19% and true negative were 31% (Table 3). However, as mentioned earlier, these values include canopy cover types that were not necessarily of interest when running the road extraction process.

To address this concern for road extraction of undesired areas, stratification based on canopy type was used to help improve identification of the values (Table 4). This resulted in a reduction of false positives by 15 percent, an increase of false negatives by one percent, and an increase in true negatives by seven percent.

The results of the road extraction process produced the following results: false positives 34%, false negatives 20%, true negatives 38%, and true positives 80%. As seen by this analysis, extreme differences in cover type throughout an area will have a large impact on the results of the road extraction process. In particular, false positives are most sensitive to these differences (Figure 10).

Table 3. Road extraction statistics for the entire study area (These statistics are biased by including all cover types not just the cover type of interest).

	False Positives	False Negatives	True Negatives	True Positives
Clear Cut or Meadow Cover Type				
Mean	20%	38%	64%	62%
STD	19%	18%	29%	18%
Min	7%	25%	44%	49%
Max	34%	51%	85%	75%
Mature Cover Type				
Mean	63%	12%	20%	88%
STD	19%	5%	17%	5%
Min	40%	4%	3%	80%
Max	88%	20%	44%	96%
Young Cover Type				
Mean	12%	27%	48%	73%
STD	NA	NA	NA	NA
Min	12%	27%	48%	73%
Max	12%	27%	48%	73%
Average				
Mean	49%	19%	31%	81%
STD	28%	14%	26%	14%
Min	7%	4%	3%	49%
Max	88%	51%	85%	96%

Table 4. Road extraction statistics for only cover types of interest.

	False Positives	False Negatives	True Negatives	True Positives
Clear Cut or Meadow Cover Type				
Mean	32%	22%	49%	78%
STD	33%	27%	33%	27%
Min	9%	2%	26%	59%
Max	56%	41%	72%	98%
Mature Cover Type				
Mean	38%	21%	38%	79%
STD	8%	13%	14%	13%
Min	27%	4%	16%	58%
Max	46%	42%	58%	96%
Young Cover Type				
Mean	6%	12%	16%	88%
STD	NA	NA	NA	NA
Min	6%	12%	16%	88%
Max	6%	12%	16%	88%
Average				
Mean	34%	20%	38%	80%
STD	16%	14%	18%	14%
Min	6%	2%	16%	58%
Max	56%	42%	72%	98%

3.2 Road Geometry Comparison

The TopCAT profile extraction process provided X, Y, and Z coordinates of evenly spaced points along the profile (Figure 11). Transects were spaced 5 meters apart and points within a transect were spaced 0.5 meters apart. This spacing provided a high resolution of the road prism compared to conventional road prism measurements, which usually only collect data points on the road edges, centerline, top of the ditch, bottom of the ditch and the top of the cut slope and the bottom of the fill slope, road transects are usually spaced between 7.62-15.24 meters apart, providing a balance between accuracy of the road geometry and speed of the survey.

With this data, road geometry variables including road width, cross-slope, and the cut or fill slope were extracted. However, the road prism was not always easy to detect in the profile, as shown by road segment 410 O D Y (Figure 12).

Even with the challenges of identifying some road prisms, the differences between the aerial and terrestrial road geometry were generally consistent. The average absolute value difference between the road width in comparing the aerial and terrestrial data was 1.1m, the average absolute difference between the cross slope and the left cut/fill slope was three percent, while the difference between the right cut/fill slopes was four percent (Table 5). These results are on par with other studies of the differences in aerial LiDAR road geometry and field measurements (Craven et al., 2011; White et al., 2010).

4. Conclusion

We developed a novel algorithm to extract forest road networks from aerial LiDAR data using intensity information and localized point densities. The road

extraction process was successful in identifying 67 percent of the roads that were field sampled. This approach proved to be generally successful in identifying gravel surface forest roads but was unsuccessful in identifying native surface forest roads. When native surface roads were removed from the analysis, the process successfully identified 84 percent of the forest roads segments by length. When considering only roads that were within the cover type of interest, this process identified 80 percent of the roads correctly.

With respect to comparing road geometry variables derived from the aerial and terrestrial LiDAR datasets, the average difference in the road width was 1.1m, the cut/fill slope differences were minimal (<4%), and the difference in road cross slope was only 2%. These results agreed well with other published results (Craven et al. 2011; White et al. 2010). The largest difference between the aerial and terrestrial LiDAR data was the resolution of data. As seen in Figure 11 (B) and Figure 12 the aerial road profile was unable to show the smaller changes in the road surface, ditch width, or road edge as made evident in the terrestrial data. The aerial data was not able to identify ruts in the running surface as seen in Figure 12.

This methodology will prove useful when trying to extract forest road geometry across the entire forest transportation network to evaluate the accessibility of non-standard vehicles. The evaluation of non-standard vehicle accessibility could aid forest landowners in determining which vehicles could be used to transport non-conventional products; providing opportunities for the forest industry to increase economic value from forests.
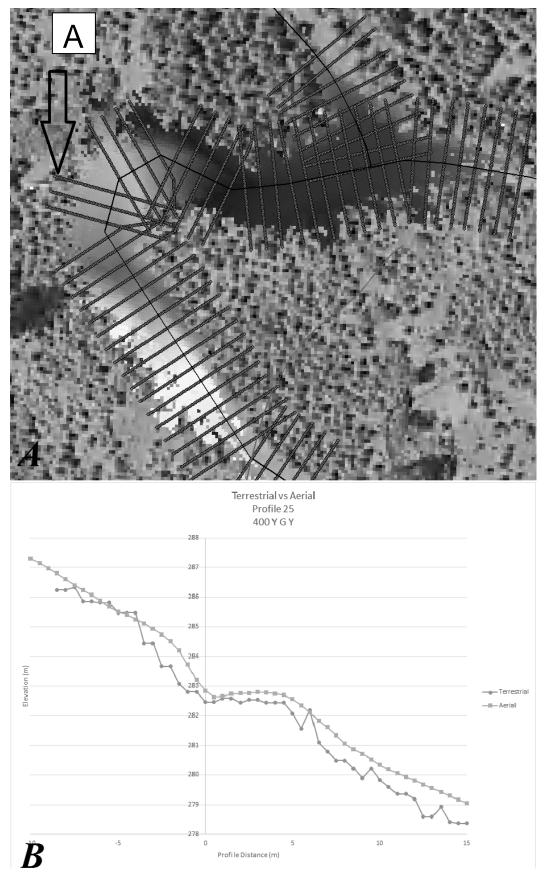
Figure 11. (A) Transects of the 400 Y G Y road segment (Overlapping transects are desired; as transects at 90 degrees to the road centerline capture the desired road geometry for evaluating vehicle accessibility), (B) A extracted road cross-sections in A (Notice the smooth aerial data and the fine terrestrial data).
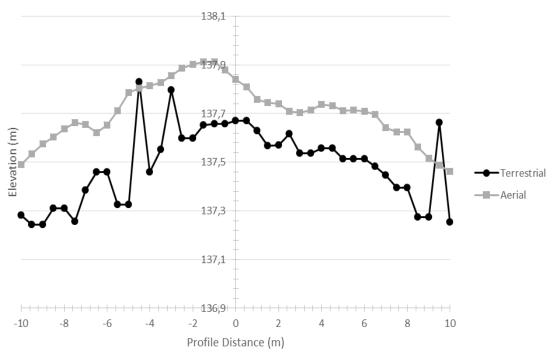
Figure 12. A road profile from road segment 410 O D Y (Notice the spikes in the terrestrial data, this is the result of using the statistical vegetation filter in a heavily grassed location).

Table 5. The summary table of the difference between the extracted road geometry variables.

	Mean	STD	Max	Min
Road Width (m)	1.1	0.2	5.5	0.1
Cross Slope	2%	2%	12%	0%
Left cut/fill slope	3%	4%	70%	0%
Right cut/fill slope	4%	5%	56%	0%

References

Beck, S., 2014. The Use of LiDAR to Identify Forest Transportation Networks. M.S. Thesis, Oregon State University, College of Forestry, Corvallis. Retrieved from Oregon State University, OR, USA.

Bourke, P., 1989. Efficient Triangulation Algorithm Suitable for Terrain Modelling. Pan Pacific Computer Conference, Beijing, China.

Craven, M., Wing, M., Sessions, J., Wimer, J., 2011. Assessment of Airborne Light Detection and Ranging (LiDAR) for use in Common Forest Engineering Geomatic Applications. M.S. Thesis, Oregon State Universtiy, College of Forestry, Corvallis. Retrieved from Oregon State University, OR, USA.

Jenson, J.R., 2007. Remote Sensing of the Environment: An Earth Resource Perspective. (J. Howard, D. Kaveney, K. Schiaparelli, & E. Thomas, Eds.) Upper Saddle River, NJ, USA.

Olsen, M., 2011. Bin 'n' grid: A simple program for statistical filtering of point cloud data.

Olsen, M.J., Young, A.P., Ashford, S.A., 2012. TopCAT- Topographical Compartment Analysis Tool to Anlyze seacliff and beach change in GIS. Computers & Geosciences, 284-292.

Rieger, W., Kerschner, M., Reiter, T., Rottensteiner, F., 1999. Roads and buildings from laser scanner data within a forest enterprise. International Archives of Photogrammetry and Remote Sensing, 32(3), W14.

Soler, T., Michalak, P., Weston, N.D., Snay, R. A., Foote, R. H. 2006. Accuracy of OPUS solutions for 1-h to 4-h observing sessions. *GPS solutions*, 10(1), 45-55.

Watershed Sciences., 2008. LiDAR Remote Sensing Data Collection: McDonald-Dunn Research Forest. Corvallis, OR, USA.

White, R. A., Dietterick, B.C., Mastin, T., Strohman, R., 2010. Forest Roads Mapped Using LiDAR in Steep Forested Terrain. *Remote Sensing*, 2(4):1120-1141.